Separation and Purification Technology 253 (2020) 117502

Contents lists available at ScienceDirect

Separation and Purification Technology

journal homepage: www.elsevier.com/locate/seppur

Complete process for the selective recovery of textile dyes using aqueous two-phase system

L.V.T.D. Alencar[a], L.M.S. Passos[a], M.A.R. Martins[b], I.M.A. Barreto[a], C.M.F. Soares[a,c], A.S. Lima[a,c], R.L. Souza[a,c,*]

[a] UNIT – Tiradentes University, Av. Murilo Dantas 300, Farolândia, Aracaju-SE, Brazil
[b] CICECO – Aveiro Institute of Materials, Department of Chemistry, University of Aveiro, 3810-193 Aveiro, Portugal
[c] ITP – Technology and Research Institute, Av. Murilo Dantas, 300, Aracaju-SE, Brazil

ARTICLE INFO

Keywords:
Aqueous two-phase systems
Textile dyes
Ionic liquids
Kamlet-Taft parameters
Recycling

ABSTRACT

Environmental problems arising from the release of dyes through industrial aqueous effluents are an emerging concern. To mitigate the problem, this work provides an experimental study on the use of aqueous two-phase systems (ATPS) for the selective separation and posterior recovery of dyes. Additionally, the complete recycling of the phase forming components is achieved. Azo dyes used in real textile industries, Direct Red 80 - DR80 and Direct Yellow 86 - DY86, were used. An initial screening of the ATPS forming elements was performed and the ATPS composed of 63 wt% acetonitrile (ACN) + 20 wt% cholinium bitartrate ([Ch][Bit]) + water at 25 °C were selected. An extraction efficiency of around 91% of DY86 to the ACN-rich phase and of approximately 99% of DR80 to the [Ch][Bit]-rich phase was obtained. The Kamlet-Taft parameters of the ATPS coexisting phases were measured aiming to understand the partitioning mechanism, especially for the migration of DY86 to the ACN-rich phase. The recovery of the DR80 from [Ch][Bit]-rich phase was of about 93% using a chitosan adsorbent (1:75, m/v) under constant stirring and at 45 °C, while ACN was completely recovered by evaporation. It was herein demonstrated that an ATPS based on a common organic solvent and a cholinium-based ionic liquid has potential for the separation and recovery of textile dyes.

1. Introduction

Dyes are some of the most significant aquatic pollutants discharged by industry. Worldwide, it is estimated that more than 7×10^5 tonnes per year of wastewater containing dyes are generated by industries [1–3]. One of the main sources of dye-contaminated wastewater are the textile industries, which involve the consumption of various types of dyes [4–6]. Currently, there are more than 100,000 different commercially available dyes [3,7]. Most of the textile dyes belong to the azo group that accounts for 60–70% of all the dye groups [8,9]. In general, azo dyes have a chromophoric azo group (−N=N−) attached to at least one but usually two aromatic nucleus in their structure, making them resistant to biodegradation [9,10].

An inadequate disposal of mentioned effluents can have a significant impact on the aquatic environment by altering their physical, chemical and biological properties [11–14]. This has led to an increase of stringent laws and regulations, forcing industries to find effective treatments for their industrial effluents before releasing them into the environment [15–17]. Several physical, chemical and biological treatment techniques have been proposed to remove residual dyes from water [4,12]. These techniques include separation using membranes [18,19], coagulation [20], oxidative processes [21], electrochemical treatment [22] and biological methods [11]. However, most treatment methods have limitations as the generation of hazardous waste, slow degradation rates and high costs [23–26].

In this sense, aqueous two-phase systems (ATPS) arise as an alternative to treat wastewater contaminated with dyes. ATPS are described as being an efficient technique for the recovery of compounds from both organic and inorganic origin [27,28]. Typically they are formed by mixing aqueous solutions of two immiscible solutes such as polymer + polymer, polymer + salt, salt + salt, short chain aliphatic alcohols + salt and ionic liquid (IL) + salt [29–33]. Each phase of the aqueous system is rich in one of the solutes, resulting in two aqueous phases with different chemical and physical properties. This leads to a system that can be tailored according with the desired migration of the compounds [34,35]. ATPS may be recyclable and economical viable, they involve short processing times and are scalable for application in industrial processes [36].

* Corresponding author at: Tiradentes University, Avenida Murilo Dantas 300, 49032-490 Aracaju, Sergipe, Brazil.
E-mail address: ranyere_souza@itp.org.br (R.L. Souza).

https://doi.org/10.1016/j.seppur.2020.117502
Received 7 February 2020; Received in revised form 19 June 2020; Accepted 20 July 2020
Available online 03 August 2020
1383-5866/

In recent decades, ATPS have been introduced as a promising alternative for the removal of dyes from aqueous matrices. Examples include the removal of: Remazol Yellow Gold RNL using polyethylene glycol (PEG) - ATPS [23]; Amaranth using deep eutectic solvents ([polypropylene glycol (PPG) 400]:[N_{4444}]Br – ATPS) [37]; Sudan III, Choranilic Acid and Indigo Blue using ATPS based on ILs ([P_{4444}]Cl or [P_{4444}]Br) [38]; Malachite Green, Methylene Blue and Reactive Red 195 using polyethylene oxide (PEO) - ATPS [39]; Orange II and Remazol Brilliant Blue R ([C_4bim][dca] or [C_4bim]Br - ATPS) [40], and Reactive Black 5 and Acid Black 48 using micellar-ATPS with Tween 20 [41]. In all cases, these systems have been optimized for individual dye separation reaching extraction efficiencies ≥ 98%. However, in all these works, when using two or more different dyes in a mixture, the selectivity of separation between the dyes is not observed using only one step of the ATPS. In addition, most of ATPS studies use dyes as a partition model only to understand the mechanisms of interaction and partitioning between the system phases [34,42]. When considering the development of greener cost-effective processes, only a couple of works managed to address the recycling of the ATPS components [35,38]. The recyclability of the ATPS components can represent more than 50% of the total process cost [43]. Consequently, we emphasize the importance in finding suitable ATPS for the dyes and phase forming components recovery, since still this is a challenging task towards the application ATPS in industrial processing.

Therefore, the aim of the present work was to investigate the application of ATPS for the selective separation of two azo dyes used in the dyeing process of the textile industry. An ATPS screening is initially performed, followed by studies regarding the optimal separation varying the IL anion, the solvent and the system composition. To understand the separation mechanism, the Kamlet-Taft solvatochromic parameters are addressed. In addition, the complete recycling of the phase forming components is investigated.

2. Materials and methods

2.1. Materials

The present study was carried out using poly(ethylene glycol-ran-propylene glycol) monobutyl ether (UCON, average molar mass of 3900 g.mol^{-1} and composed of 0.50 ethylene glycol and 0.50 propylene glycol), different polyethylene glycol polymers (average molecular weight of 400, 1000, 1500, 2000 and 8000 g.mol^{-1}, abbreviated as PEG 400, PEG 1000, PEG 1500, PEG 2000 and PEG 8000, respectively) and carbohydrates (sorbitol, xylitol, sucrose, fructose). Polymers and carbohydrates were supplied by Sigma–Aldrich®. Salts [potassium citrate ($C_6H_5K_3O_7$), sodium potassium tartrate ($KNaC_4H_4O_6$) and ammonium sulfate ($(NH_4)_2SO_4$)], solvents [acetonitrile (ACN), 2-propanol, 1,3-dioxolane and tetrahydrofuran (THF)] and cholines [Cholinium chloride ([Ch]Cl), cholinium bitartrate ([Ch][Bit]) and cholinium dihydrogencitrate ([Ch][DHCit])] were all purchased from Sigma–Aldrich®, with purities higher than 98 wt%. The water used was purified in a Milli-Q (Direct Q® 3UV) water purification equipment. The dyes Direct Yellow 86 (DY86, C.I. 29325) and Direct Red 80 (DR80, C.I. 35780) – chemical structure presented in Fig. 1 – were provided by a textile manufacturer located in Estância, SE, Brazil. These dyes are used during the dyeing process of the mentioned textile industry.

2.2. Experimental phase diagrams

The phase diagrams of the ATPS composed of solvents (1,3-dioxolane or 2-propanol) + cholinium-based ionic liquids ([Ch]Cl, [Ch][DHCit] or [Ch][Bit]) + water or polymer (PEG 1500 or PEG 2000) + sodium potassium tartrate + water were determined using the cloud point titration method [44]. Aqueous solutions at 90 wt% of solvents, cholinium-ionic liquids solution at 30 wt%, polymer solution at 50 wt% and sodium potassium tartrate solution at 30 wt% were prepared for the determination of the phase diagrams at 25 °C and at atmospheric pressure. The systems compositions were determined by weight quantification of all components added considering an uncertainty of ± 10^{-5} g. The experimental solubility curves were correlated and evaluated using Eq. (1) [45]:

$$w_1 = Aexp[(Bw_2^{0,5}) - (Cw_2^3)] \quad (1)$$

where w_1 and w_2 are the mass fraction percentages of the solvent and the cholinium-ionic liquids, respectively; or of the polymer and the sodium potassium tartrate, respectively. A, B and C are fitting parameters obtained by least squares regression.

2.3. Dyes partition

The partition of the dyes Direct Yellow 86 (DY86) and the Direct Red 80 (DR80) in ATPS was evaluated. The initial ATPS mixture compositions were selected based on the phase diagrams determined in this work (Fig. A.1 and Tables A.1, A.2 and A.3 in Supporting Information) and reported in the literature (Table A.4) [33,46–53]. Different combinations of ATPS phase-forming constituents were investigated (Table A.5). Each extraction system was prepared by adding approximately 2 g.L^{-1} (considering the total mixture) of each dye into a glass tube already containing the total mass of the ternary system of 5 g. The ATPS was then allowed to equilibrate at 25 °C and atmospheric pressure conditions during 24 h. The top and bottom phases were then carefully separated, and the pH of both phases measured at 25 °C using a DIGIMED DM-20 pH meter. The dyes were then quantified in both phases through UV spectroscopy (wavelength: 397 nm for DY86 and 528 nm for DR80) using a HACH DR-5000 spectrometer. Possible interferences from the phase promoters (solvents and ILs) were taken into account and found to be of no significance at the dilution levels used. Additionally, the influence of the presence of DY86 on the spectrophotometric analysis of DR80 was evaluated by analysing the concentration of DR80 in standard solutions containing different amounts of DY86. The influence of the presence of DR80 on the spectrophotometric analysis of DY86 was also assessed. The relative error associated with the quantifications was < 5%. At least three samples of each extraction system were prepared, being the dyes precisely quantified in both aqueous phases. The partition coefficients of both dyes ($K_{DR80orDY86}$) were determined using Eq. (2):

$$K_{DR80orDY86} = \frac{C_T}{C_B} \quad (2)$$

where C_T and C_B are the dye concentration in the top and bottom phases, respectively.

The dye selectivities (S) were calculated by the ratio of the partition coefficients of each dye in the same system. In order to evaluate the dye extraction efficiencies for top phase (EE_T, %) and bottom phase (EE_B, %) and the volume ratio (R_v) in each ATPS, the following equations were used:

$$R_V = \frac{V_T}{V_B} \quad (3)$$

$$EE_T, \% = \frac{100}{1 + \left(\frac{1}{R_V \times K_{DR80orDY86}}\right)} \quad (4)$$

$$EE_B, \% = \frac{100}{1 + R_V \times K_{DR80orDY86}} \quad (5)$$

where V is the phase volume, and T and B refers to the top and bottom phases, respectively.

2.4. Kamlet-Taft parameters

The solvatochromic probes *N,N*-diethyl-4-nitroaniline and 4-nitroaniline were used to determine the dipolarity/polarizability (π*) and

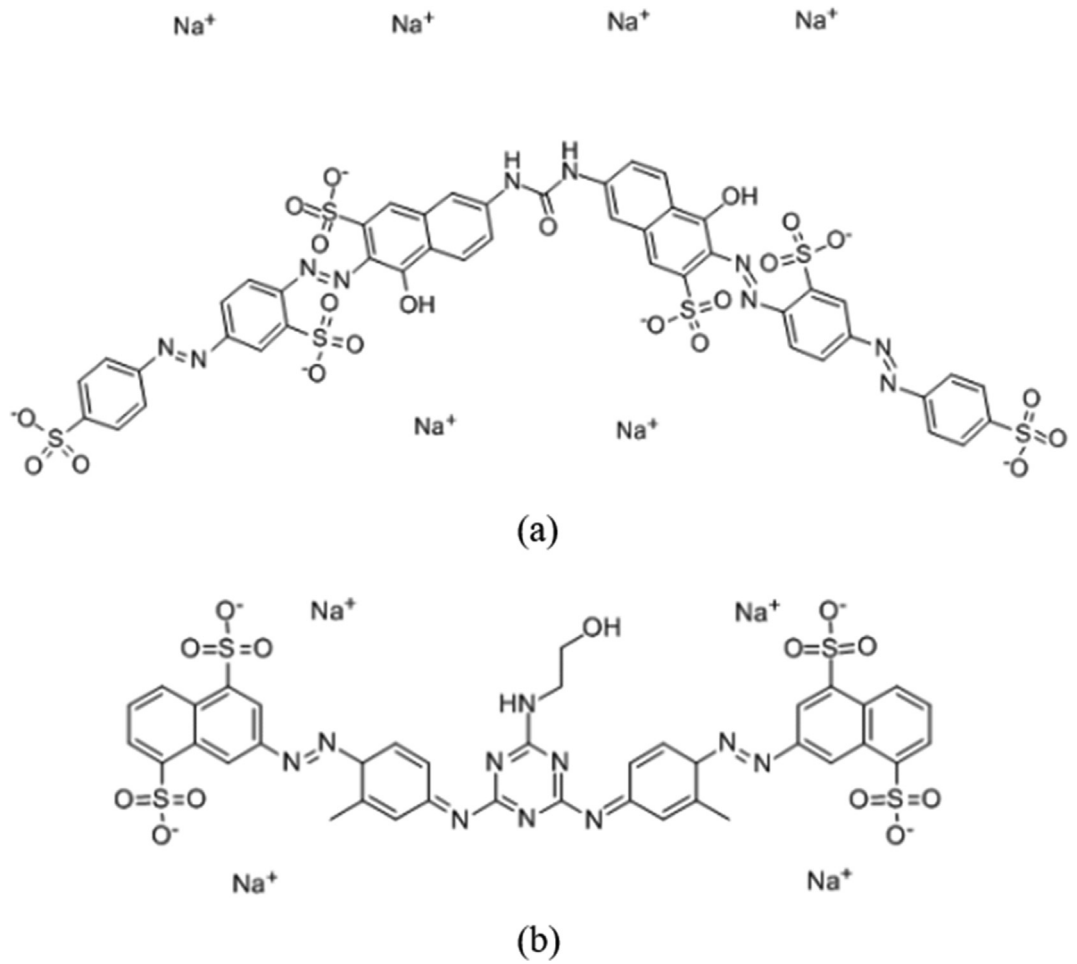

Fig. 1. Chemical structure of the dyes: (a) Direct Red 80 and (b) Direct Yellow 86.

hydrogen-bond acceptor abilities (β), respectively, of the coexisting phases of the studied ATPS at 25 °C. Small quantities of the probes (≈0.30 mg) were added to each phase that were then stirred in a vortex mixer, and scanned by a HACH DR-5000 spectrometer at 25 °C. The longest wavelength absorption band of each probe in each phase was determined. For each mixture, a total of three replicates were prepared. The π* and β solvatochromic parameters were determined by the following equations:

$$\pi^* = \frac{\nu_{N,N\,(phase)} - \nu_{N,N\,(cyclohexane)}}{\nu_{N,N\,(DMSO)} - \nu_{N,N\,(cyclohexane)}} \tag{6}$$

$$\beta = \frac{(\Delta\nu_{N,N\,(phase)} - \Delta\nu_{N,N\,(cyclohexane)}) \times 0.76}{\Delta\nu_{N,N\,(DMSO)} - \Delta\nu_{N,N\,(cyclohexane)}} \tag{7}$$

$$\Delta\nu = \Delta\nu_{N,N} - \Delta\nu_{4N} \tag{8}$$

$$\nu = \frac{1}{\lambda_{maxprobe}} \times 10^{-4} \tag{9}$$

where ν is the the experimental wavenumber and$\lambda_{maxprobe}$ is the maximum wavelength of the probe, the subscripts *N,N* and *4 N* represent the solvatochromic probes *N,N*-diethyl-4-nitroaniline and 4-nitroaniline, respectively; while *cyclohexane* and *DMSO* correspond to the values for these standard solvents and *phase* to the value for the phase of ATPS investigated.

2.5. Recovery of phase forming components

After achieving an effective dyes separation using ATPS, additional experiments were carried out to evaluate of recovery of the dyes and phase forming components. The removal of the dye DR80 from the ATPS phase after separation was performed through its adsorption onto chitosan. The adsorbent was prepared with chitosan that was obtained from crab shell according to the procedure reported by Barreto et al. [54]. Adsorption experiments were realized with a solid–liquid ratio of 1:150 g.mL^1 between chitosan (g) and the bottom phase (mL) of the ATPS composed of 63 wt% of ACN + 20 wt% of [Ch][Bit] + 0.2 wt% of each dye (DR80 and DY86) + water, at 25 °C. To evaluate the effect of agitation on the adsorption performance of DR80, experiments were performed by three different methods (lasting 60 h of analysis): constant stirring (at 250 rpm), vigorously stirring for 1 min (in vortex mixer) and without agitation. The effect of the adsorbent dosage was studied by varying the solid–liquid ratio 1:300; 1:150; 1:100 and 1:75 g.mL^{-1} (250 rpm, 25 °C). Additionally, three temperatures (25, 35 and 45 °C) where investigated at a fixed solid–liquid ratio (1:75 g.mL^{-1}) and at constant stirring 250 rpm. All experiments were made in triplicate and the data analysis was performed with the average experimental values.

The concentration of DR80 dye was determined by UV spectroscopy using a HACH DR-5000 spectrometer, at the maximum absorption wavelength of 528 nm. The dye removal percentage was calculated by Eq. (10):

$$Dyeremoval\,(\%) = \frac{C_0 - C_e}{C_0} \times 100 \tag{10}$$

where C_0 and C_e are the initial and final concentrations of the dye in the liquid phase, respectively.

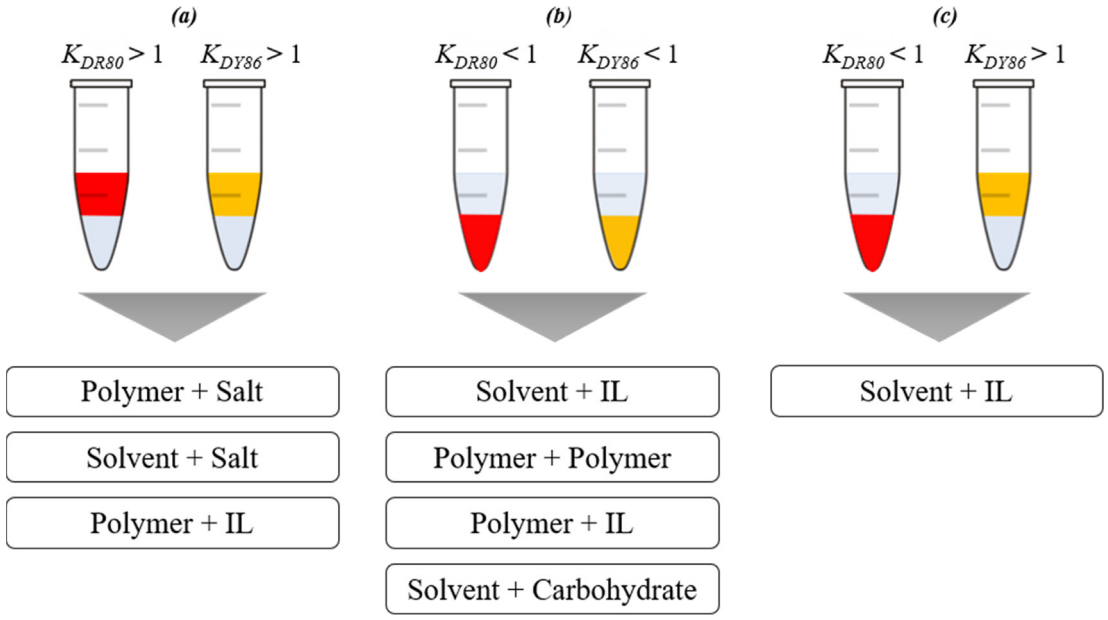

Fig. 2. Screening of ATPS formed by the combination of several constituents (polymers, salts, carbohydrates, ionic liquids (IL) and solvents) in relation to the partitioning of the dyes: Direct Red 80 (K_{DR80}) and Direct Yellow 86 (K_{DY86}).

3. Results and discussion

3.1. ATPS screening for dyes separation

The ATPS separation efficiency depends on the properties of the compounds to be extracted as well as on the properties of the compounds that form the ATPS [42,55,56]. Thus, a screening of constituents to form the ATPS, capable of selectively separate the two textile dyes DR80 and DY86, was initially performed and is schematically represented in Fig. 2 and listed in Table A.5. In total, 27 different combinations of ATPS phase-forming components were investigated. A volume ratio (R_V) of approximately 1.00 ± 0.06 was used in all systems. The resultant volume ratios were compared, ensuring that similar experimental conditions.

As shown in Table A.5, ATPS based on potassium, sulfate and sodium salts promoted the migration of both dyes into a single phase (PEG or 2-propanol rich phase), due to their high *salting-out* capacity [34,37]. Systems formed by acetonitrile and carbohydrates (sorbitol, xylitol, sucrose or fructose), PEG and copolymer (UCON) or PEG and cholinium-based ionic liquid were also not able to selectively separate the dyes, even using polymers with different molecular masses (400, 1000 and 8000 g.mol^{-1}). Both dyes migrate for the more hydrophilic phases rich in carbohydrate (acetonitrile-carbohydrates ATPS) [52,53] and rich in PEG (PEG-UCON ATPS) [51]. These results may be explained by the similarity between the chemical structures of the dyes (Fig. 1) and by their relative hydrophobicity, measured by the partition in the 1-octanol/water system, log *P*, (-0.97 and −7.28 for DY86 and DR80, respectively [57]). In systems formed by PEG and cholinium-based ionic liquids, the dye partition (DY86 and DR80) occurs not only for the PEG phase (top phase), but also for the bottom phase when choline chloride is used. In these systems, the migration of dyes is ruled by forces that are not exclusively due to a hydrophobicity balance.

The selective separation of the investigated dyes was only possible using ATPS based on organic solvents (ACN and 2-propanol) and ILs (Fig. 2c and Table A.5). Among the many investigated ATPS, only those can provide the most appropriate interaction mechanism for the separation. Is therefore a challenge to find an ATPS capable of mediating a selective separation process for these two dyes.

3.2. Dyes partition

To identify and optimize the best conditions for the separation of DY86 and DR80 textile dyes, three parameters were evaluated: IL anion, solvent and system composition.

3.2.1. Effect of the IL anion

First, ATPS composed of acetonitrile and cholinium-based ionic liquids were evaluated. In search of a better selectivity and dye partitioning, three different ionic liquids ([Ch]Cl, [Ch][DHCit] and [Ch][Bit]) were investigated – Fig. 3. Partition coefficients and extraction efficiencies are shown in Table A.6 (Support Information). The initial composition of the mixtures were selected taking into consideration the biphasic regions of the phase diagrams for each cholinium-based ionic liquid and acetonitrile at 25 °C previously reported by our research group [49].

Fig. 3 (a) show that there is practically no change in the partitioning of DR80 across the three ATPS investigated. DR80 partitions almost completely to the more hydrophilic phase, the bottom phase (rich in IL, $K_{DR80} < 1$). This is due to the strong hydrophilic interactions between the dye and the cholinium-salts, as predicted by their distribution coefficients, log *D* (-4.6; −4.8; −3.1 and −6.9 for [Ch]Cl, [Ch][DHCit], [Ch][Bit] and DR80, respectively) [57]. In addition, according to the pH of the phases and the DR80 speciation curve shown in the Table A.7 and Fig. A.2 (Support Information), respectively, the DR80 dye remains ionized with the negative charge (-6) in all pH (3.69 to 4.46) investigated.

Although all cholinium-based ionic liquids studied have a hydrophilic character, as predicted by their distribution coefficients, the migration of the DY86 dye (log *D* −2.15) [57] is not mainly controlled by the hydrophobic/hydrophilic balance of the phases, as showed in Fig. 3 (b). Results show that the partition of DY86 (K_{DY86}) increases to the acetonitrile-rich phase when the systems formed by [Ch][DHCit] and [Ch][Bit] are used, from 0.04 ± 0.01 with [Ch]Cl, to 0.35 ± 0.01 and 2.24 ± 0.02 with [Ch][DHCit] and [Ch][Bit], respectively. Table A.8 lists the DY86 speciation (Fig. A.3) between the phases of the different systems. It is possible to observe that the negatively charged dye structures are reduced following the trend of [Ch]Cl > [Ch][DHCit] > [Ch][Bit]. Therefore, electrostatic interactions are expected to be reduced, leading the DY86 partition to the more neutral (ACN-

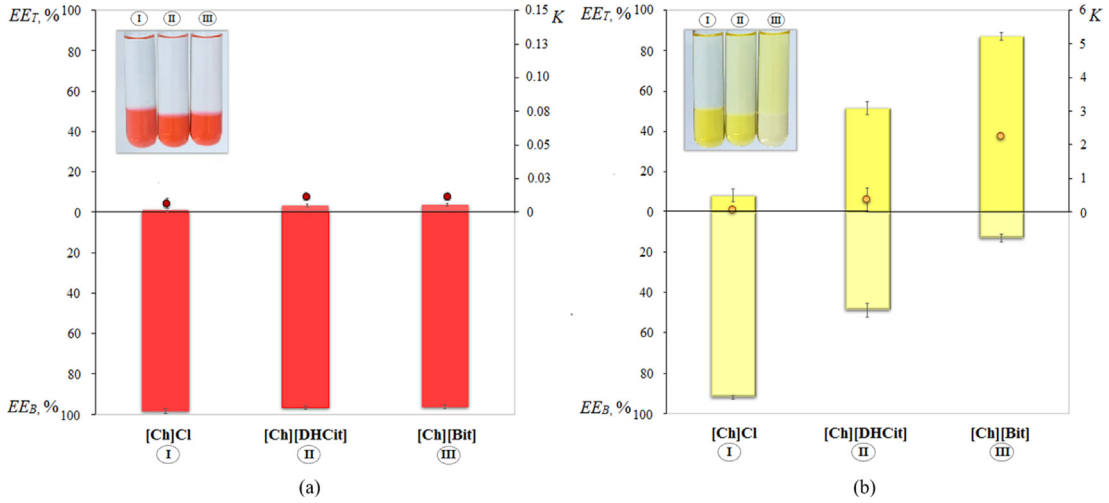

Fig. 3. Extraction efficiencies in the top phase (EE_T, % - represented by the bars) and in the bottom phase (EE_B, % - represented by the bars) and partition coefficient (K - represented by the circles) of dyes (a) DR80 and (b) DY86 by applying ATPS composed of 63 wt% of ACN + 11 wt% of cholinium-based ionic liquids + 0.2 wt% of dye + water, at 25 °C and atmospheric pressure.

rich) phase. Thus, from the investigated ILs, the one that presents greater selectivity for the DR80 and DY86 dyes is the [Ch][Bit] based ATPS (Table A.6). To better understand the partition mechanisms, the solvatochromic parameters of the phases of the studied systems are analysed below.

3.2.1.1. Kamlet-Taft parameters. A commonly used scale to characterize solvents in terms of solvatochromic parameters is the multiparameter scale of Kamlet and Taft [58–60]. This approach consists on the use of a set of solvatochromic probes which allow the assessment of different interactions for the same solvent, such as its dipolarity/polarizability (π*) and hydrogen-bond acceptor abilities (β) [58–60]. This approach has been successfully used for the description of solutes partition in ATPS composed of polymers and salts [61–63], and salts and ionic liquids [64].

Aiming to further understand the partition of dyes in the herein studied ATPS, Kamlet-Taft parameters of the coexisting phases of 63 wt % of ACN + 11 wt% of different cholinium-ionic liquids + water were determined. Inhere "solvent" refers to the global phase mixture, and not to an individual component, such as water, ACN or ionic liquid. The results obtained for π* and β are presented in Table 1.

From the results obtained it is possible to see that independently of the IL used, the IL-rich phases always present higher dipolarity/polarizability values when compared to the ACN-rich phases. Furthermore, in the IL-rich phase π* follows the trend [Ch][Bit] < [Ch][DHCit] < [Ch]Cl, while in the ACN-rich phase the opposite trend is observed – Fig. 4. This behaviour seems to promote a larger partition of DY86 dye into the top phase (ACN-rich phase).

By the other side, β of the IL-rich phase follows the trend [Ch][Bit] > [Ch][DHCit] > [Ch]Cl while in the ACN-rich phase it decreases in the same order (Table 1 and Fig. 4). Since the β parameter describes the hydrogen-bond acceptor ability, this also seems to promote a larger affinity of DY86 dye to the ACN-rich phase through the formation of hydrogen bonds, since interactions by Van Der Waals are the main fixation mechanism of this type of dye on substrates [65]. Greater selectivity was observed for the system composed of [Ch][Bit] when compared to those formed by [Ch]Cl or [Ch][DHCit] (Table A.6).

Despite these differences of the Kamlet-Taft parameters between the coexisting phases of the investigated ATPS, the DR80 partitions almost completely to the bottom (rich in IL, $K_{DR80} < 1$) in the three ATPS investigated. This result supports the above observation that hydrophilic interaction was one of the main driving forces for the partition of the DR80 dye.

ATPS constituted by cholinium-based ionic liquids and ACN show a considerably broad variation of both non-specific and specific interactions, suggesting that this type of systems could be seen as a good option for the separation of molecules and compounds in which their partition could be ruled by specific interactions. Furthermore, these differences are strongly dependent on the anion of the ionic liquids investigated suggesting that cholinium-based ATPS can be tuned for the enhanced and selective extraction of a specific solute.

3.2.2. Effect of solvent

Due to the low viscosity of the phases that results in short time separations, ATPS based on organic solvents have been nominated as an efficient alternative when compared to polymer-based ATPS [36,66,67].

Among the ILs investigated, [Ch][Bit] was the one leading to higher partition coefficients (Fig. 3). Therefore, the solvent effect in dyes partition was evaluated using [Ch][Bit] combined with water and the organic solvents 1,3-dioxolane, THF, 2-propanol and ACN.

The initial mixture compositions were selected taking into account the phase diagrams reported in the literature [49,50] or herein measured (Table A.2 and Table A.3). The extraction results are presented in Fig. 5. All partition coefficients and extraction efficiencies of the dyes in these ATPS are shown in Table A.9.

Solvents with heterocyclic structures, THF and 1,3-dioxolane, seem to interact less strongly with the dyes evaluated in this work, as both

Table 1
Kamlet–Taft parameters between the coexisting phases of 63 wt% of ACN + 11 wt% of different cholinium-based ionic liquids + water at 25 °C and atmospheric pressure.

ATPS	Π^*_{ACN}	Π^*_{IL}	β_{ACN}	β_{IL}
[Ch]Cl	0.917 ± 0.016	1.076 ± 0.019	0.290 ± 0.023	0.585 ± 0.034
[Ch][DHCit]	0.857 ± 0.015	1.144 ± 0.002	0.389 ± 0.027	0.497 ± 0.026
[Ch][Bit]	0.810 ± 0.007	1.200 ± 0.022	0.562 ± 0.017	0.283 ± 0.030

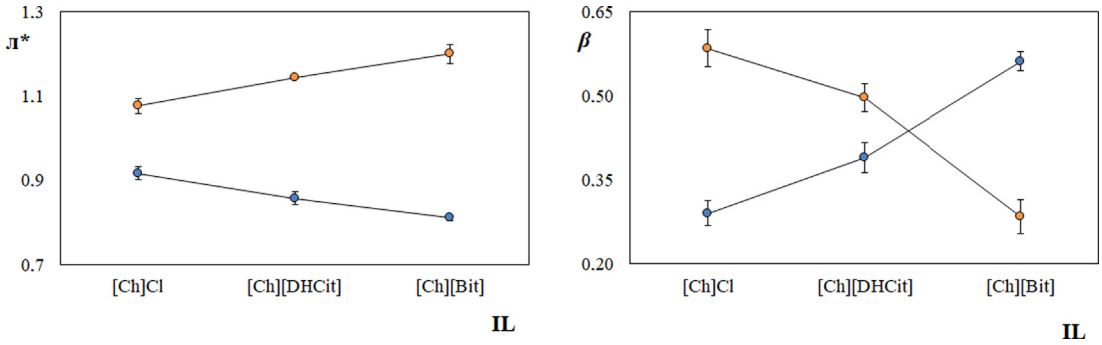

Fig. 4. Kamlet-Taft parameters for ATPS composed of 63 wt% of ACN + 11 wt% of different cholinium-based ionic liquids + water, at 25 °C and atmospheric pressure: ACN-rich phase (●); IL-rich phase (●).

dyes preferentially partition to bottom phase (K < 1, IL-rich phase). This is most evident for the partitioning of the DR80 dye (Fig. 5a), which has a more hydrophilic character compared to DY86 (log *P* is −0.97 and −7.28 for DY86 and DR80, respectively [57]). Besides the hydrophilic interactions between the dyes and [Ch][Bit], entropic effects may also influence partition [68]. Despite the similarity between the chemical structures of the two dyes, DR80 is larger when compared to DY86 (1373 Da and 1066 Da, respectively) [57], what may decrease its solubility in the linear solvents. This is evident, even for solvents with different chemical structures, such as 1,3-dioxolane (heterocyclic structure) and ACN (linear structure), which have close hydrophilic capacity (reflected by the polar surface area and log *P* data – Table A.10), since an inversion of the partition of the DY86 from the bottom (in 1,3-dioxolane-ATPS) to the top phase (in ACN-ATPS) is observed (Fig. 5b).

Systems composed of solvents with linear structures, such as ACN and 2-propanol, led to a more efficient partition of DY86 dye to the solvent-rich phase (K_{DY86} = 1.54 ± 0.1 and $EE_{T,\ DY86}$ = 88.63 ± 1.79 for 2-propanol; and K_{DY86} = 2.24 ± 0.2 and $EE_{T,\ DY86}$ = 87.02 ± 0.12 for ACN) while DR80 dye partitions almost completely to the bottom phase (IL-rich phase, K_{DR80} < 1).

As shown in Fig. 5 (a), in the ATPS composed of 2-propanol there is a significant partitioning of the DR80 for the top phase (K_{DR80} = 0.12 ± 0.01), which reduces the selectivity (Table A.9). Among the solvents evaluated, 2-propanol is the only that has hydrogen bond donors in its structure [57], what leads to strong interactions between 2-propanol and the two direct dyes, due to Van Der Waals interactions [65].

In short, the ATPS based in ACN and [Ch][Bit] showed the highest selectivity for the investigated dyes (Table A.9). Due to their physicochemical properties, such as low viscosity, high resolution and low boiling point [69], ACN is one of the most preferred organic solvents for use in various separations techniques, including ATPS applications [49,70,71].

3.2.3. Composition of the system

ATPS based in [Ch][Bit] + ACN showed the greater selectivity for the two textile dyes investigated (Table A.9). Thus, the next step is to evaluate the effect of phase forming components concentration. All partition coefficient and extraction efficiency data of the dyes in the studied ATPS are shown in Table A.11 (in Support Information).

Fig. 6 (a) shows the effect of ACN concentration (43–70 wt%) on the partition coefficient and extraction efficiencies of the dyes. As ACN concentration increases from 43 to 63 wt%, K_{DY86} also increases from 1.31 ± 0.04 to 2.24 ± 0.02, and the EE_T of DY86 increases from 34.42 ± 2.66 to 87.02 ± 0.12. It is important to highlight that 63 wt % ACN is the limit concentration at which one have the best DY86 partition in the top phase. At higher concentrations of ACN, water has little effect on hydrogen bond networks [72], which reduces its availability for the ACN-rich phase. Thus, a decrease in the migration of the DY86 dye to the ACN-rich phase is expected.

To evaluate the effect of concentration of [Ch][Bit] (7–20 wt%) on dye partitioning, the concentration of 63 wt% of ACN in ATPS was fixed. Fig. 6 (b) shows that as the concentration of [Ch][Bit] increases from 7 to 20 wt%, the K_{DY86} increases from 1.27 ± 0.08 to 3.43 ± 0.11, respectively. As expected, the increase in the concentration of [Ch][Bit] increased K_{DY86} and EE_T% of DY86 due to the *salting-out* effect [34,37]. For [Ch][Bit] concentrations above 20 wt%,

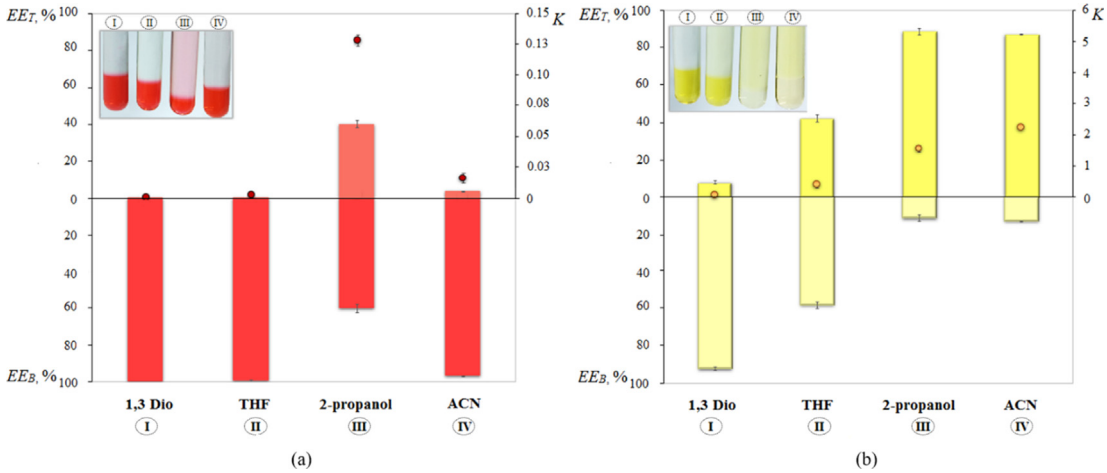

Fig. 5. Extraction efficiency in the top phase (EE_T, % - represented by the bars) and the bottom phase (EE_B, % - represented by the bars) and partition coefficient (*K* - represented by the symbols) of dyes (a) DR80 and (b) DY86 by applying systems composed of 63 wt% of different solvents + 11 wt% of [Ch][Bit] + 0.2 wt% of dye + water, at 25 °C and atmospheric pressure.

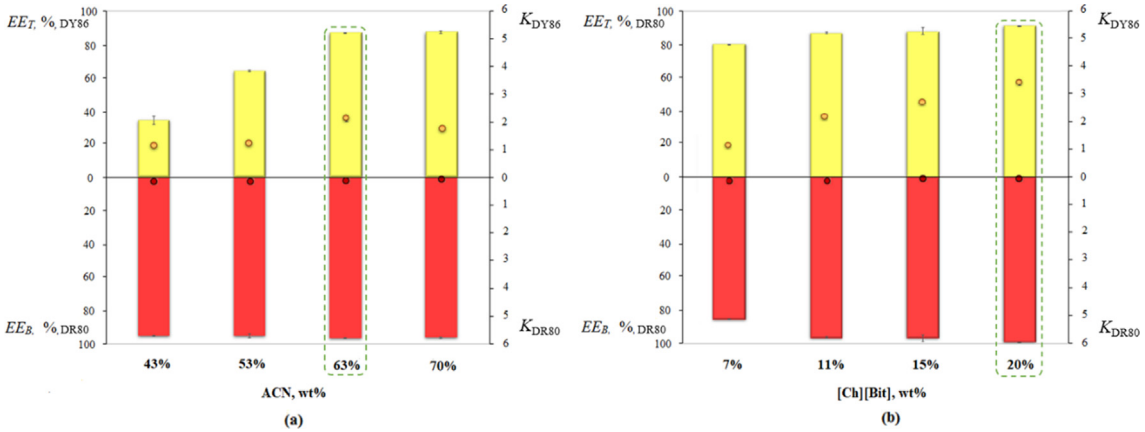

Fig. 6. Extraction efficiency in the top phase (EE_T, % - represented by the bars) and the bottom phase (EE_B, % - represented by the bars) and partition coefficient (K - represented by the symbols) of dyes DR80 and DY86 by applying ATPS composed of: (a) different ACN concentrations (43; 53; 63 and 70 wt%) + 11 wt% of [Ch][Bit] + 0.2 wt% of each dye + water and (b) 63 wt% of ACN + different [Ch][Bit] concentrations (7; 11; 15 and 20 wt%) + 0.2 wt% of each dye + water, at 25 °C and atmospheric pressure.

the formation of ATPS does not occur due to the formation of a third solid phase (IL precipitation in the system). Below 7 wt%, the system enters the monophasic regime, as predicted by the binodal curve [49]. As previously discussed, DR80 has a strong hydrophilic character (log P is −7.28 [57]) and therefore remained almost constant (in the bottom phase) for all the concentrations evaluated.

The most effective dye separation were obtained in ATPS composed of 63 wt% of ACN + 20 wt% of [Ch][Bit] + water. This system has potential in the separation process of textile dyes with a selective extraction of S = 1143.3 (Table A.11) and high extraction efficiencies: EE_T of DY86 of 91.05 ± 0.16% to the ACN-rich phase, and EE_B of DR80 of 99.09 ± 1.13% to the [Ch][Bit]-rich phase. Additionally, a fast phase separation of approximately 23 s was observed with the ACN-based ATPS.

In addition, aiming to increase ATPS attractiveness at industrial levels, their potential for scaling up was investigated. A scaling up from 5 to 100 g of total mass of the ATPS composed of 63 wt% of ACN + 20 wt% of [Ch][Bit] + 0.2 wt% of each dye (DR80 and DY86) + water was performed. Results are shown in Fig. 7 and the partition coefficient and extraction efficiency data listed in Table A.12. The ATPS based on ACN and [Ch][Bit] was scaled up with the same

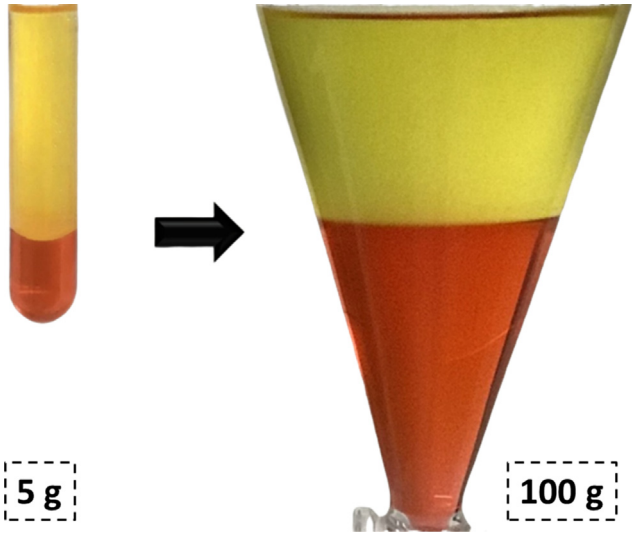

Fig. 7. Scaling up from 5 to 100 g of total mass of the ATPS composed of 63 wt % of ACN + 20 wt% of [Ch][Bit] + 0.2 wt% of each dye (DR80 and DY86) + water, at 25 °C and atmospheric pressure.

performance at all scales with a recovery medium yield of 91.58 ± 0.35% and 99.1. ± 0.06% for DY86 and DR80, respectively. These findings modestly indicate that the systems under study have considerable potential for use in extraction/purification process at industrial scale.

3.3. Recovery of phase forming components

Aiming at the development of a cost-effective and sustainable process, additional experiments were carried out to evaluate the possibility of dyes recovery and the recyclability of the phase forming components ([Ch][Bit] and ACN). After the complete partitioning of DY86 to the ACN-rich phase and DR80 to [Ch][Bit]-rich phase, each phase was carefully separated. For the top-phase (ACN-rich phase), it is here proposed the recycling of the phase components by the evaporation of acetonitrile. Acetonitrile has a high vapor pressure (97.1 hPa at 20.0 °C [57]) that favours its recovery step, which requires approximately 5 min using a rotary evaporator at 40 °C. After the removal of the dye from the solvent, the acetonitrile can be directly reintroduced in the preparation of a new ATPS.

DR80 removal from the [Ch][Bit] rich phase was performed using a chitosan adsorption process. Chitosan is a biocompatible and biodegradable polymer, used in a wide range of applications including dye removal from industrial effluents [73]. When selecting the experimental details, our first criteria was to choose conditions with economic industrial applicability. Thus, we evaluated: the stirring mode - experiments without agitation (to reduce large-scale costs) in comparison with agitation at 250 rpm and vigorous agitation (in Vortex); the solid–liquid ratio (m/v) between adsorbent (g) and lower phase (mL) of ATPS considering the maximum conditions of solid (adsorbent) saturation in the liquid (dye solution); the temperature variation between 25 and 45 °C, *i.e.*, close to the ambient temperature. The results are shown in the Fig. 8.

From Fig. 8 (a) it can be concluded that after 60 h the dye removal is more efficient when using constant agitation (250 rpm) (82.5 ± 1.8%), when compared with vigorous stirring for 1 min (55.0 ± 3.3%) or without agitation (42.2 ± 1.4%). During the agitation process the chitosan boundary-layer resistance decreases and the system mobility increases, increasing the adsorption capacity [74]. Regardless of the ratio of adsorbent mass to dye volume, the adsorption capacity of chitosan increases as a function of time in all cases - Fig. 8 (b). However, as the solid ratio in the liquid increases (maximum of 1:75, m/v), the percentage of dye removal increases corresponding to a maximum of (93.2 ± 0.8%) recovery after 60 h and for 1:75 (m/v). Such trend is mostly attributed to an increase in the adsorptive surface

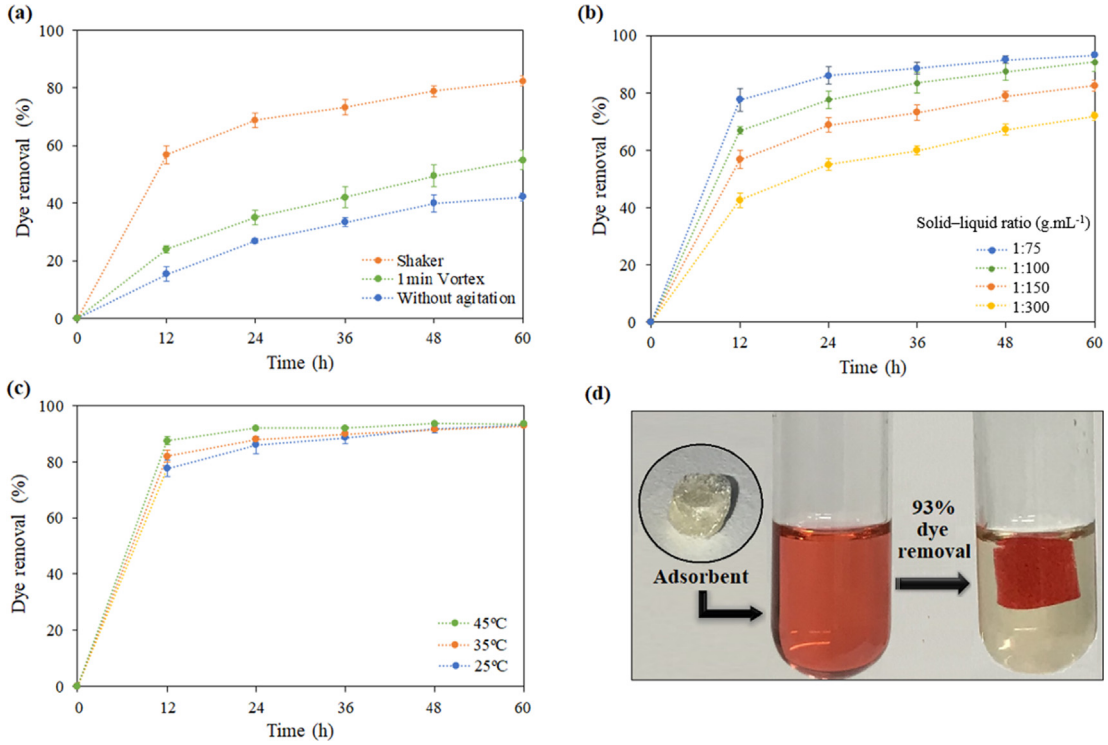

Fig. 8. %DR80 dye adsorption onto chitosan: (a) effect of agitation, (b) effect of solid–liquid ratio, (c) effect of temperature, (d) IL-rich phase before and after the removal of 93% of DR80 through its adsorption onto chitosan.

area and the availability of more active adsorption sites [75]. The effect of temperature during the adsorption process was also evaluated. An increase from 25 °C to 45 °C promotes an increase in dye removal from 77.6 ± 2.8% to 87.4 ± 1.4%, respectively, after 12 h with constant stirring (250 rpm). This effect is probably due to the increase of the available space on the chitosan surface, thus providing additional active sites for dye adsorption [76]. Overall, chitosan can be considered as an affective adsorbent to remove dye DR80. Thus, the ACN present in the top phase and the IL present in the bottom phase can be reused for a new application cycle, promoting a sustainable development of the process.

4. Conclusions

ATPS were successfully applied for the selective separation of two textiles dyes (Direct Yellow 86 and Direct Red 80). From the initial optimization study performed, the best ATPS components and processing conditions were selected. The ATPS composed of 63 wt% ACN + 20 wt% [Ch][Bit] + water at 25 °C was selected. Extraction efficiencies of DY86 of 91.05 ± 0.16% to the ACN-rich phase, and of DR80 of 99.09 ± 1.13% to the [Ch][Bit]-rich phase were obtained. This ATPS was successfully scaled up and is characterized by short processing times. The phase forming components were successfully recycled and the dyes isolated. The system under study has great potential to be applied in the recovery of dyes from textile industry.

Declaration of Competing Interest

The authors declare that they have no known competing financial interests or personal relationships that could have appeared to influence the work reported in this paper.

Acknowledgments

The authors acknowledge the financial support of Coordenação de Aperfeiçoamento de Pessoal de Nível Superior (CAPES), Brazil - Finance Code 001; and Conselho Nacional de Desenvolvimento Científico e Tecnológico (CNPq - 426956/2016-8), Brazil. M.A.R.M acknowledges the project CICECO, Portugal, Institute of Materials, UIDB/50011/2020 & UIDP/50011/2020, financed by national funds through the FCT/MEC and when appropriate co-financed by FEDER under the PT2020 Partnership Agreement.

Appendix A. Supplementary data

Supplementary data to this article can be found online at https://doi.org/10.1016/j.seppur.2020.117502.

References

[1] Z. Hasan, S.H. Jhung, Removal of hazardous organics from water using metal-organic frameworks (MOFs): Plausible mechanisms for selective adsorptions, J. Hazard. Mater. 283 (2015) 329–339, https://doi.org/10.1016/j.jhazmat.2014.09.046.
[2] S. Rajoriya, S. Bargole, S. George, V.K. Saharan, Treatment of textile dyeing industry effluent using hydrodynamic cavitation in combination with advanced oxidation reagents, J. Hazard. Mater. 344 (2018) 1109–1115, https://doi.org/10.1016/j.jhazmat.2017.12.005.
[3] I.R. Zamora-Garcia, A. Alatorre-Ordaz, J.G. Ibanez, J.C. Torres-Elguera, K. Wrobel, S. Gutierrez-Granados, Efficient degradation of selected polluting dyes using the tetrahydroxoargentate ion, Ag(OH)4 −, in alkaline media, Chemosphere 191 (2018) 400–407, https://doi.org/10.1016/j.chemosphere.2017.10.041.
[4] H.A. Rahman, N. Jusoh, N. Othman, M.B. Rosly, R.N.R. Sulaiman, N.F.M. Noah, Green formulation for synthetic dye extraction using synergistic mixture of acid-base extractant, Sep. Purif. Technol. 209 (2019) 293–300, https://doi.org/10.1016/j.seppur.2018.07.053.
[5] J. Rovira, J.L. Domingo, Human health risks due to exposure to inorganic and organic chemicals from textiles: A review, Environ. Res. 168 (2019) 62–69, https://doi.org/10.1016/j.envres.2018.09.027.
[6] T. Hussain, A. Wahab, A critical review of the current water conservation practices in textile wet processing, J. Clean Prod. 198 (2018) 806–819, https://doi.org/10.1016/j.jclepro.2018.07.051.
[7] J. Abdi, M. Vossoughi, N.M. Mahmoodi, I. Alemzadeh, Synthesis of metal-organic framework hybrid nanocomposites based on GO and CNT with high adsorption capacity for dye removal, Chem. Eng. J. 326 (2017) 1145–1158, https://doi.org/10.1016/j.cej.2017.06.054.
[8] S. Chatterjee, S. Chatterjee, B.P. Chatterjee, A.K. Guha, Adsorptive removal of

congo red, a carcinogenic textile dye by chitosan hydrobeads: Binding mechanism, equilibrium and kinetics, Colloid. Surface. A 299 (2007) 146–152, https://doi.org/10.1016/j.colsurfa.2006.11.036.
[9] A.E. Ghaly, R. Ananthashankar, M. Alhattab, V. vasudevan ramakrishnan, Production, characterization and treatment of textile effluents: A critical review, J. Chem. Eng. Process. Technol., 5 (2014) 1000182. https://doi.org/10.4172/2157-7048.1000182.
[10] C. Wang, A. Yediler, D. Lienert, Z. Wang, A. Kettrup, Toxicity evaluation of reactive dyestuffs, auxiliaries and selected effluents in textile finishing industry to luminescent bacteria Vibrio fischeri, Chemosphere 46 (2002) 339–344, https://doi.org/10.1016/S0045-6535(01)00086-8.
[11] P.M. Dellamatrice, M.E. Silva-Stenico, L.A.B.d. Moraes, M.F. Fiore, R.T.R. Monteiro, Degradation of textile dyes by cyanobacteria, Braz. J. Microbiol., 48 (2017) 25–31. https://doi.org/10.1016/j.bjm.2016.09.012.
[12] G. Patra, R. Barnwal, S.K. Behera, B.C. Meikap, Removal of dyes from aqueous solution by sorption with fly ash using a hydrocyclone, J. Environ. Chem. Eng. 6 (2018) 5204–5211, https://doi.org/10.1016/j.jece.2018.08.011.
[13] L. Hossain, S.K. Sarker, M.S. Khan, Evaluation of present and future wastewater impacts of textile dyeing industries in Bangladesh, Environ. Dev. 26 (2018) 23–33, https://doi.org/10.1016/j.envdev.2018.03.005.
[14] U. Roy, S. Sengupta, P. Banerjee, P. Das, A. Bhowal, S. Datta, Assessment on the decolourization of textile dye (Reactive Yellow) using Pseudomonas sp. immobilized on fly ash: Response surface methodology optimization and toxicity evaluation, J. Environ. Manage., 223 (2018) 185–195. https://doi.org/10.1016/j.jenvman.2018.06.026.
[15] C. Hessel, C. Allegre, M. Maisseu, F. Charbit, P. Moulin, Guidelines and legislation for dye house effluents, J. Environ. Manage. 83 (2007) 171–180, https://doi.org/10.1016/j.jenvman.2006.02.012.
[16] L. Liu, J. Zhang, Y. Tan, Y. Jiang, M. Hu, S. Li, Q. Zhai, Rapid decolorization of anthraquinone and triphenylmethane dye using chloroperoxidase: Catalytic mechanism, analysis of products and degradation route, Chem. Eng. J. 244 (2014) 9–18, https://doi.org/10.1016/j.cej.2014.01.063.
[17] S. Vajnhandl, J.V. Valh, The status of water reuse in European textile sector, J. Environ. Manage. 141 (2014) 29–35, https://doi.org/10.1016/j.jenvman.2014.03.014.
[18] N. Othman, R.N. Raja Sulaiman, H.A. Rahman, N.F.M. Noah, N. Jusoh, M. Idroas, Simultaneous extraction and enrichment of reactive dye using green emulsion liquid membrane system, Environ. Technol. 40 (2019) 1476–1484, https://doi.org/10.1080/09593330.2018.1424258.
[19] N. Othman, S.N. Zailani, N. Mili, Recovery of synthetic dye from simulated wastewater using emulsion liquid membrane process containing tri-dodecyl amine as a mobile carrier, J. Hazard. Mater. 198 (2011) 103–112, https://doi.org/10.1016/j.jhazmat.2011.10.014.
[20] M.R. Gadekar, M.M. Ahammed, Coagulation/flocculation process for dye removal using water treatment residuals: modelling through artificial neural networks, Desalin. Water Treat. 57 (2016) 26392–26400, https://doi.org/10.1080/19443994.2016.1165150.
[21] S. Martínez-López, C. Lucas-Abellán, A. Serrano-Martínez, M.T. Mercader-Ros, N. Cuartero, P. Navarro, S. Pérez, J.A. Gabaldón, V.M. Gómez-López, Pulsed light for a cleaner dyeing industry: Azo dye degradation by an advanced oxidation process driven by pulsed light, J. Clean Prod. 217 (2019) 757–766, https://doi.org/10.1016/j.jclepro.2019.01.230.
[22] N.P. Shetti, S.J. Malode, R.S. Malladi, S.L. Nargund, S.S. Shukla, T.M. Aminabhavi, Electrochemical detection and degradation of textile dye Congo red at graphene oxide modified electrode, Microchem. J. 146 (2019) 387–392, https://doi.org/10.1016/j.microc.2019.01.033.
[23] J.M. Alvarenga, R.A. Fideles, M.V. Silva, G.F. Murari, J.G. Taylor, L.R. Lemos, G. Dias Rodrigues, A.B. Mageste, Partition study of textile dye Remazol Yellow Gold RNL in aqueous two-phase systems, Fluid Phase Equilib., 391 (2015) 1–8. https://doi.org/10.1016/j.fluid.2015.01.022.
[24] P.V. Nidheesh, R. Gandhimathi, S.T. Ramesh, Degradation of dyes from aqueous solution by Fenton processes: a review, Environ. Sci. Pollut. R. 20 (2013) 2099–2132, https://doi.org/10.1007/s11356-012-1385-z.
[25] V. Katheresan, J. Kansedo, S.Y. Lau, Efficiency of various recent wastewater dye removal methods: A review, J. Environ. Chem. Eng. 6 (2018) 4676–4697, https://doi.org/10.1016/j.jece.2018.06.060.
[26] A. Sinha, S. Lulu, V. S, S. Banerjee, S. Acharjee, W.J. Osborne, Degradation of reactive green dye and textile effluent by Candida sp. VITJASS isolated from wetland paddy rhizosphere soil, J. Environ. Chem. Eng., 6 (2018) 5150–5159. https://doi.org/10.1016/j.jece.2018.08.004.
[27] M. González-González, M. Rito-Palomares, Aqueous two-phase systems strategies to establish novel bioprocesses for stem cells recovery, Crit. Rev. Biotechnol. 34 (2014) 318–327, https://doi.org/10.3109/07388551.2013.794125.
[28] A. Hamta, M.R. Dehghani, Application of polyethylene glycol based aqueous two-phase systems for extraction of heavy metals, J. Mol. Liq. 231 (2017) 20–24, https://doi.org/10.1016/j.molliq.2017.01.084.
[29] M. Baghlani, R. Sadeghi, The capability of tetra alkyl ammonium bromides for aqueous biphasic systems formation with both polymers and electrolytes in aqueous solutions, Fluid Phase Equilib. 465 (2018) 34–47, https://doi.org/10.1016/j.fluid.2018.03.002.
[30] C.M.S.S. Neves, S. Shahriari, J. Lemus, J.F.B. Pereira, M.G. Freire, J.A.P. Coutinho, Aqueous biphasic systems composed of ionic liquids and polypropylene glycol: insights into their liquid–liquid demixing mechanisms, Phys. Chem. Chem. Phys. 18 (2016) 20571–20582, https://doi.org/10.1039/C6CP04023C.
[31] J.F.B. Pereira, K.A. Kurnia, M.G. Freire, J.A.P. Coutinho, R.D. Rogers, Controlling the Formation of Ionic-Liquid-based Aqueous Biphasic Systems by Changing the Hydrogen-Bonding Ability of Polyethylene Glycol End Groups, ChemPhysChem 16 (2015) 2219–2225, https://doi.org/10.1002/cphc.201500146.
[32] G.D. Rodrigues, M.d.C.H. Silva, L.H.M. Silva, L.S. Teixeira, V.M. Andrade, Liquid − Liquid Phase Equilibrium of Triblock Copolymer L64, Poly(ethylene oxide-b-propylene oxide-b-ethylene oxide), with Sulfate Salts from (278.15 to 298.15) K, J. Chem. Eng. Data, 54 (2009) 1894–1898. https://doi.org/10.1021/je9000685.
[33] M.G. Sanglard, F.O. Farias, F.H.B. Sosa, T.P.M. Santos, L. Igarashi-Mafra, M.R. Mafra, Measurement and correlation of aqueous biphasic systems composed of alcohol (1-propanol/2-propanol/tert-butanol) + (NH4)2SO4 + H2O at 298 K and a textile dye partition, Fluid Phase Equilib. 466 (2018) 7–13, https://doi.org/10.1016/j.fluid.2018.03.009.
[34] R.L. Souza, V.C. Campos, S.P.M. Ventura, C.M.F. Soares, J.A.P. Coutinho, Á.S. Lima, Effect of ionic liquids as adjuvants on PEG-based ABS formation and the extraction of two probe dyes, Fluid Phase Equilib. 375 (2014) 30–36, https://doi.org/10.1016/j.fluid.2014.04.011.
[35] X. Wu, Y. Liu, Y. Zhao, K.-L. Cheong, Effect of Salt Type and Alkyl Chain Length on the Binodal Curve of an Aqueous Two-Phase System Composed of Imidazolium Ionic Liquids, J. Chem. Eng. Data 63 (2018) 3297–3304, https://doi.org/10.1021/acs.jced.8b00188.
[36] M.A. Torres-Acosta, K. Mayolo-Deloisa, J. González-Valdez, M. Rito-Palomares, Aqueous Two-Phase Systems at Large Scale: Challenges and Opportunities, Biotechnol. J. 14 (2019) 1800117, https://doi.org/10.1002/biot.201800117.
[37] H. Zhang, Y. Wang, Y. Zhou, J. Chen, X. Wei, P. Xu, Aqueous biphasic systems formed by deep eutectic solvent and new-type salts for the high-performance extraction of pigments, Talanta 181 (2018) 210–216, https://doi.org/10.1016/j.talanta.2018.01.014.
[38] A.M. Ferreira, J.A.P. Coutinho, A.M. Fernandes, M.G. Freire, Complete removal of textile dyes from aqueous media using ionic-liquid-based aqueous two-phase systems, Sep. Purif. Technol. 128 (2014) 58–66, https://doi.org/10.1016/j.seppur.2014.02.036.
[39] G.A. Borges, L.P. Silva, J.A. Penido, L.R. de Lemos, A.B. Mageste, G.D. Rodrigues, A method for dye extraction using an aqueous two-phase system: Effect of co-occurrence of contaminants in textile industry wastewater, J. Environ. Manage. 183 (2016) 196–203, https://doi.org/10.1016/j.jenvman.2016.08.056.
[40] A. Dimitrijević, A. Jocić, N. Zec, A. Tot, S. Papović, S. Gadžurić, M. Vraneš, T. Trtić-Petrović, Improved single-step extraction performance of aqueous biphasic systems using novel symmetric ionic liquids for the decolorisation of toxic dye effluents, J. Ind. Eng. Chem. 76 (2019) 500–507, https://doi.org/10.1016/j.jiec.2019.04.017.
[41] N. Escudero, F.J. Deive, M.Á. Sanromán, M.S. Álvarez, A. Rodríguez, Design of eco-friendly aqueous two-phase systems for the efficient extraction of industrial finishing dyes, J. Mol. Liq. 284 (2019) 625–632, https://doi.org/10.1016/j.molliq.2019.04.011.
[42] A.B. Mageste, T.D.A. Senra, M.C.H. da Silva, R.C.F. Bonomo, L.H.M. Silva, Thermodynamics and optimization of norbixin transfer processes in aqueous biphasic systems formed by polymers and organic salts, Sep. Purif. Technol. 98 (2012) 69–77, https://doi.org/10.1016/j.seppur.2012.06.012.
[43] P.A.J. Rosa, A.M. Azevedo, S. Sommerfeld, W. Bäcker, M.R. Aires-Barros, Aqueous two-phase extraction as a platform in the biomanufacturing industry: Economical and environmental sustainability, Biotechnol. Adv. 29 (2011) 559–567, https://doi.org/10.1016/j.biotechadv.2011.03.006.
[44] R.L. Souza, R.A. Lima, J.A.P. Coutinho, C.M.F. Soares, Á.S. Lima, Novel aqueous two-phase systems based on tetrahydrofuran and potassium phosphate buffer for purification of lipase, Process. Biochem. 50 (2015) 1459–1467, https://doi.org/10.1016/j.procbio.2015.05.015.
[45] J.C. Merchuk, B.A. Andrews, J.A. Asenjo, Aqueous two-phase systems for protein separation: Studies on phase inversion, J. Chromatogr. B Biomed. Sci. Appl. 711 (1998) 285–293, https://doi.org/10.1016/S0378-4347(97)00594-X.
[46] S.C. Silvério, A. Wegrzyn, E. Lladosa, O. Rodríguez, E.A. Macedo, Effect of Aqueous Two-Phase System Constituents in Different Poly(ethylene glycol)–Salt Phase Diagrams, J. Chem. Eng. Data 57 (2012) 1203–1208, https://doi.org/10.1021/je2012549.
[47] M. Jayapal, I. Regupathi, T. Murugesan, Liquid − Liquid Equilibrium of Poly(ethylene glycol) 2000 + Potassium Citrate + Water at (25, 35, and 45) °C, J. Chem. Eng. Data, 52 (2007) 56–59. https://doi.org/10.1021/je060209d.
[48] J.F.B. Pereira, K.A. Kurnia, O.A. Cojocaru, G. Gurau, L.P.N. Rebelo, R.D. Rogers, M.G. Freire, J.A.P. Coutinho, Molecular interactions in aqueous biphasic systems composed of polyethylene glycol and crystalline vs. liquid cholinium-based salts, Phys. Chem. Chem. Phys. 16 (2014) 5723–5731, https://doi.org/10.1039/C3CP54907K.
[49] P.L. Santos, L.N.S. Santos, S.P.M. Ventura, R.L. Souza, J.A.P. Coutinho, C.M.F. Soares, Á.S. Lima, Recovery of capsaicin from Capsicum frutescens by applying aqueous two-phase systems based on acetonitrile and cholinium-based ionic liquids, Chem. Eng. Res. Des. 112 (2016) 103–112, https://doi.org/10.1016/j.cherd.2016.02.031.
[50] R.L. Souza, R.A. Lima, J.A.P. Coutinho, C.M.F. Soares, Á.S. Lima, Aqueous two-phase systems based on cholinium salts and tetrahydrofuran and their use for lipase purification, Sep. Purif. Technol. 155 (2015) 118–126, https://doi.org/10.1016/j.seppur.2015.05.021.
[51] P.P. Madeira, J.A. Teixeira, E.A. Macedo, L.M. Mikheeva, B.Y. Zaslavsky, ΔG(CH2) as solvent descriptor in polymer/polymer aqueous two-phase systems, J. Chromatogr. A 1185 (2008) 85–92, https://doi.org/10.1016/j.chroma.2008.01.035.
[52] G.B. Cardoso, T. Mourão, F.M. Pereira, M.G. Freire, A.T. Fricks, C.M.F. Soares, Á.S. Lima, Aqueous two-phase systems based on acetonitrile and carbohydrates and their application to the extraction of vanillin, Sep. Purif. Technol. 104 (2013) 106–113, https://doi.org/10.1016/j.seppur.2012.11.001.

[53] G.B. Cardoso, I.N. Souza, T. Mourão, M.G. Freire, C.M.F. Soares, Á.S. Lima, Novel aqueous two-phase systems composed of acetonitrile and polyols: Phase diagrams and extractive performance, Sep. Purif. Technol. 124 (2014) 54–60, https://doi.org/10.1016/j.seppur.2014.01.004.
[54] I.M.A. Barreto, P.A. Lima, C.M.F. Soares, R.L. Souza, A.S. Lima (2018). Brazilian Patent No. BR 1020180132598.
[55] C.M. Junqueira, D. Silva Cabral, J.A. Penido, A.B. Mageste, L.S. Virtuoso, How does the use of surfactants in polymer-salt based aqueous two-phase systems affect the annatto dye (Bixa orellana L.) partitioning?, Fluid Phase Equilib., 478 (2018) 14–22. https://doi.org/10.1016/j.fluid.2018.08.013.
[56] H. Passos, D.J.P. Tavares, A.M. Ferreira, M.G. Freire, J.A.P. Coutinho, Are Aqueous Biphasic Systems Composed of Deep Eutectic Solvents Ternary or Quaternary Systems?, ACS Sustain. Chem. Eng., 4 (2016) 2881–2886. https://doi.org/10.1021/acssuschemeng.6b00485.
[57] Chemspider, The free chemical database, in, 2020. https://www.chemspider.com.
[58] M.J. Kamlet, R.W. Taft, The solvatochromic comparison method. I. The.beta.-scale of solvent hydrogen-bond acceptor (HBA) basicities, J. Am. Chem. Soc. 98 (1976) 377–383, https://doi.org/10.1021/ja00418a009.
[59] M.J. Kamlet, J.L.M. Abboud, M.H. Abraham, R.W. Taft, Linear solvation energy relationships. 23. A comprehensive collection of the solvatochromic parameters,pi.*,alpha., and.beta., and some methods for simplifying the generalized solvatochromic equation, J. Org. Chem. 48 (1983) 2877–2887, https://doi.org/10.1021/jo00165a018.
[60] R.W. Taft, M.J. Kamlet, The solvatochromic comparison method. 2. The.alpha.-scale of solvent hydrogen-bond donor (HBD) acidities, J. Am. Chem. Soc. 98 (1976) 2886–2894, https://doi.org/10.1021/ja00426a036.
[61] J.G. Huddleston, H.D. Willauer, R.D. Rogers, The solvatochromic properties, α, β, and π*, of PEG-salt aqueous biphasic systems, Phys. Chem. Chem. Phys. 4 (2002) 4065–4070, https://doi.org/10.1039/B203018G.
[62] O. Rodríguez, S.C. Silvério, P.P. Madeira, J.A. Teixeira, E.A. Macedo, Physicochemical Characterization of the PEG8000-Na2SO4 Aqueous Two-Phase System, Ind. Eng. Chem. Res. 46 (2007) 8199–8204, https://doi.org/10.1021/ie070473f.
[63] R.L.S. França do Rosário, R.L. Souza, F.O. Farias, M.R. Mafra, C.M.F. Soares, H. Passos, J.A.P. Coutinho, Á.S. Lima, Acetonitrile as adjuvant to tune polyethylene glycol + K3PO4 aqueous two-phase systems and its effect on phenolic compounds partition, Sep. Purif. Technol., 223 (2019) 41–48. https://doi.org/10.1016/j.seppur.2019.04.062.
[64] H. Passos, T.B.V. Dinis, E.V. Capela, M.V. Quental, J. Gomes, J. Resende, P.P. Madeira, M.G. Freire, J.A.P. Coutinho, Mechanisms ruling the partition of solutes in ionic-liquid-based aqueous biphasic systems – the multiple effects of ionic liquids, Phys. Chem. Chem. Phys. 20 (2018) 8411–8422, https://doi.org/10.1039/C8CP00383A.
[65] C.C.I. Guaratini, M.V.B. Zanoni, Corantes têxteis, Quím. Nova 23 (2000) 71–78, https://doi.org/10.1590/S0100-40422000000100013.
[66] N.E.C. Cienfuegos, P.L. Santos, A.R. García, C.M.F. Soares, A.S. Lima, R.L. Souza, Integrated process for purification of capsaicin using aqueous two-phase systems based on ethanol, Food Bioprod. Process. 106 (2017) 1–10, https://doi.org/10.1016/j.fbp.2017.08.005.
[67] M. Taha, I. Khoiroh, M.-J. Lee, Phase Behavior and Molecular Dynamics Simulation Studies of New Aqueous Two-Phase Separation Systems Induced by HEPES Buffer, J. Phys. Chem. B 117 (2013) 563–582, https://doi.org/10.1021/jp305516g.
[68] H.-O. Johansson, G. Karlström, F. Tjerneld, C.A. Haynes, Driving forces for phase separation and partitioning in aqueous two-phase systems, J. Chromatogr. B Biomed. Sci. Appl. 711 (1998) 3–17, https://doi.org/10.1016/S0378-4347(97)00585-9.
[69] E. Nemati-Kande, H. Shekaari, Salting-out effect of sodium, potassium, carbonate, sulfite, tartrate and thiosulfate ions on aqueous mixtures of acetonitrile or 1-methyl-2-pyrrolidone: A liquid–liquid equilibrium study, Fluid Phase Equilib. 360 (2013) 357–366, https://doi.org/10.1016/j.fluid.2013.09.028.
[70] C. Zhang, K. Huang, P. Yu, H. Liu, Sugaring-out three-liquid-phase extraction and one-step separation of Pt(IV), Pd(II) and Rh(III), Sep. Purif. Technol. 87 (2012) 127–134, https://doi.org/10.1016/j.seppur.2011.11.032.
[71] G.B. Cardoso, I.N. Souza, M.M. Pereira, L.P. Costa, M.G. Freire, C.M.F. Soares, Á.S. Lima, Poly(vinyl alcohol) as a novel constituent to form aqueous two-phase systems with acetonitrile: Phase diagrams and partitioning experiments, Chem. Eng. Res. Des. 94 (2015) 317–323, https://doi.org/10.1016/j.cherd.2014.08.009.
[72] S. Stehle, A.S. Braeuer, Hydrogen Bond Networks in Binary Mixtures of Water and Organic Solvents, J. Phys. Chem. B 123 (2019), https://doi.org/10.1021/acs.jpcb.9b02829.
[73] A. Srinivasan, T. Viraraghavan, Decolorization of dye wastewaters by biosorbents: A review, J. Environ. Manage. 91 (2010) 1915–1929, https://doi.org/10.1016/j.jenvman.2010.05.003.
[74] G.L. Dotto, L.A.A. Pinto, Adsorption of food dyes onto chitosan: Optimization process and kinetic, Carbohydr. Polym. 84 (2011) 231–238, https://doi.org/10.1016/j.carbpol.2010.11.028.
[75] S. Chowdhury, P. Saha, Sea shell powder as a new adsorbent to remove Basic Green 4 (Malachite Green) from aqueous solutions: Equilibrium, kinetic and thermodynamic studies, Chem. Eng. J. 164 (2010) 168–177, https://doi.org/10.1016/j.cej.2010.08.050.
[76] L. Zhang, L. Sellaoui, D. Franco, G.L. Dotto, A. Bajahzar, H. Belmabrouk, A. Bonilla-Petriciolet, M.L.S. Oliveira, Z. Li, Adsorption of dyes brilliant blue, sunset yellow and tartrazine from aqueous solution on chitosan: Analytical interpretation via multilayer statistical physics model, Chem. Eng. J. 382 (2020) 122952, , https://doi.org/10.1016/j.cej.2019.122952.